Acta Cryst. (1979). B35, 530–538

Structural Relationships Between β-Gallia, Rutile, Hollandite, Psilomelane, Ramsdellite and Gallium Titanate Type Structures

BY L. A. BURSILL

School of Physics, University of Melbourne, Parkville, Victoria 3052, *Australia*

(*Received* 13 *July* 1978; *accepted* 26 *October* 1978)

Abstract

The relationships between the above structure types are considered theoretically. New types of tunnel structures and transformation mechanisms are derived. The analysis predicts many variations of the hollandite structure type previously unsuspected. These go some way towards explaining the indefinite structural results obtained using X-ray diffraction techniques for hollandite and related minerals and also for γ-manganese oxides and hydroxides. It is strongly suggested that preparative and characterization techniques need to be far more thorough and penetrating than those used so far, if significant measurements of physical properties, such as superionic conductivity, are to be made.

1. Introduction

Wadsley (1964) first pointed out that the BX_2 framework of the hollandite-type structure is constructed of elements of the rutile (TiO_2) structure (Fig. 1*a*,*b*). The relationship may be formally described using a rotation operation (Bursill & Hyde, 1972; Hyde, Bagshaw, O'Keeffe & Andersson, 1974). Columns consisting of groups of four linear strings of octahedra parallel to c_r are rotated cooperatively, alternately clockwise and anticlockwise, through $\pi/4$ radian. The columns, which shared octahedral corners in rutile (Fig. 1*a*), now share octahedral edges in hollandite (Fig. 1*b*) in such a way that the stoichiometry remains BX_2. The large squares in Fig. 1(*b*), bound by double-octahedral strings, are empty tunnels. These provide potential sites for ions or molecules of appropriate size and charge. These sites have simple cubic eightfold coordination (Fig. 1*c*) and if they are all filled the ternary ionic compound has formula $A_2B_8X_{16}$ or $A_{0.25}BX_2$.

It is clear from the careful X-ray diffraction studies of hollandite-type minerals by Byström & Byström (1950) and phase analyses of manganese oxides (Wadsley & Walkley, 1951) that there is a wide variety of ill-defined structures related to hollandite. Often water may occur in the tunnels as well as a variety of foreign ions, such as Pb^{2+}, Ba^{2+}, K^+, Rb^+,

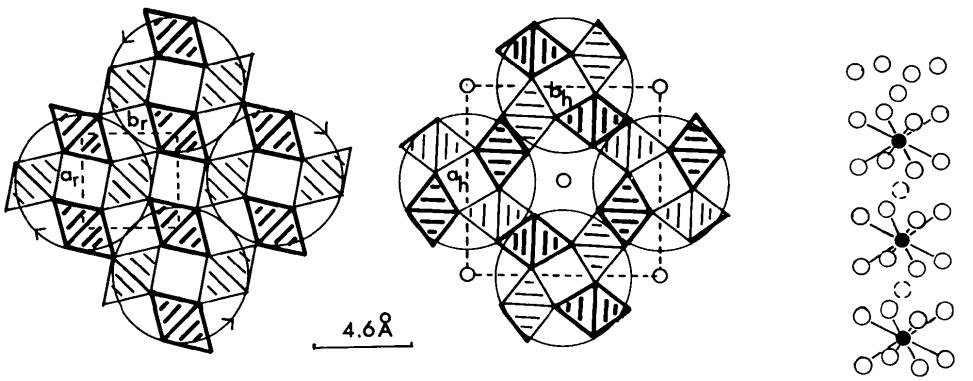

Fig. 1. (*a*) Rutile structure in $[001]_r$ projection. $[MO_6]$ octahedra share edges along projection axis forming strings which are linked by corner sharing. (*b*) Hollandite structure, $[001]_h$ projection. Double-octahedral, edge-shared chains cooperate to form large tunnels containing metals in cubic coordination. Note the corresponding rutile-like columns (circled) linking the hollandite tunnels. Rotation of circled columns in (*a*) by $\pi/4$ radian, alternately clockwise and anticlockwise, generates the hollandite structure. (*c*) Series of interstitial sites having cubic coordination. These are assumed to be alternately filled and empty in $Ba_{1.0}Mg_{1.0}Ti_7O_{16}$. The oxygens (larger open circles) are part of the framework structure shown in (*b*).

0567-7408/79/030530-09$01.00

Cs^+, *etc.* Wadsley (1964) suggested that some of these may be disordered structures of inhomogeneous structure and composition.

It occurred to us that such structures could not be completely characterized by use of X-ray diffraction techniques alone. This has been confirmed by high-resolution electron microscopy and diffraction studies of a number of hollandite specimens in this laboratory. The microstructure of hollandites is complex and many variations of the basic tetragonal structure (Fig. 1*b*) occur. As a first stage in our analysis of such structures image-matching techniques were developed to determine the optimum electron-optical requirements for imaging all of the metal atoms (spacings 2·7 to 5·4 Å) in the tetragonal projection of hollandite (Bursill & Wilson, 1977). These calculations assumed that most of the variations in the basic structure would be due to variations in filling and ordering of the *A* ions in the tunnels. However, comparison of the results for hollandite and those obtained for gallium titanates (Stone & Bursill, 1977; Lloyd, Grey & Bursill, 1976) suggested that there were also changes in the framework or host structure which could be simply explained in terms of the relationships between rutile, hollandite, β-gallia and the gallium titanate structures.

In this paper the structural relationships between these and some other structure types are considered theoretically. New structure types, intergrowth and defect structures are proposed. Following papers (Bursill & Netherway, 1979; Bursill & Stone, 1979*a*,*b*) discuss our experimental observations of variations of the hollandite and gallium titanate structures.

2. Structural background

(*a*) *Hollandite group of structures*

This structure (Fig. 1*b*) was found for a group of minerals: hollandite, cryptomelane and coronadite, which with α-MnO_2 form an isostructural series of general formula $A_{2-y}B_{8-z}X_{16}$ (Byström & Byström, 1950). *A* represents large ions such as Ba^{2+}, Pb^{2+}, or K^+, Cs^+, Rb^+ and possibly NH_4^+; *B* is Mn^{4+}, Fe^{3+} or Mn^{2+} and *X* is O^{2-} or OH^-. In the compounds studied $0{\cdot}8 < y < 1{\cdot}3$ and $0{\cdot}1 < z < 0{\cdot}5$. It is reasonable to expect that some large *A* ions are necessary to prevent collapse of the framework. α-MnO_2 for example can be prepared only in the presence of a large ion such as K^+. The cubic coordinated sites in the tunnels are seldom more than half-filled but may be almost entirely empty [Buser, Graf & Feitknecht (1954) reported the α-MnO_2 structure retained for a K^+:Mn^{4+} ratio of 1:70].

Byström & Byström (1950) studied natural minerals and reported a range of unit cells for the series hollandite, cryptomelane and coronadite. For example, one specimen was found to contain two hollandites with cell parameters, $a = 9{\cdot}91$, $b = 2{\cdot}872$, $c = 9{\cdot}75$ Å, $\beta = 90{\cdot}6°$, $V = 278{\cdot}0$ Å^3 and $a = 10{\cdot}00$, $b = 2{\cdot}879$, $c = 9{\cdot}72$ Å, $\beta = 91{\cdot}1°$, $V = 278{\cdot}8$ Å^3 respectively.

Powder photographs of cryptomelane and coronadite showed no deviations from tetragonal symmetry and the cell parameters were reported as $a = 9{\cdot}84$, $c = 2{\cdot}858$ Å and $a = 9{\cdot}89$, $c = 2{\cdot}862$ Å respectively.

Byström & Byström (1950) determined atomic coordinates for their hollandite samples by ignoring departures from tetragonal symmetry, and assuming the fractional atomic coordinates were the same for both tetragonal and pseudotetragonal cells. The unit cell contains one formula unit of $A_{2-y}B_{8-z}X_{16}$.

When deformed, the short axis becomes the monoclinic *b* axis. The deviaiton of β from 90° is from 0·5 to 1·5° and the difference $a_m - c_m$ is 0·1 to 0·2 Å. The *A* ion is surrounded by eight O atoms at 2·74 Å distance, forming cubic coordination. There are four further oxygens at 3·31 Å at the same *z* level as the *A* ions (see Fig. 1*c*). The *B* ions are surrounded by six oxygens forming octahedra with mean *B*—O distance 1·98 Å. *y* and *z* have been observed to vary from $0{\cdot}8 < y < 1{\cdot}3$ and $0{\cdot}1 < z < 0{\cdot}5$ respectively.

Single crystals of the isomorphous phase $Ba_x(Ti_{8-x}Mg_x)O_{16}$, $0{\cdot}67 < x < 1{\cdot}14$, were studied by Dryden & Wadsley (1958). They reported no departure from tetragonal symmetry with cell parameters $a = 10{\cdot}110$, $c = 2{\cdot}986$ Å. Their fractional atomic coordinates are virtually identical with those found by Byström & Byström (1950), see Table 1.

Dryden & Wadsley (1958) reported diffuse supplementary spectra, the positions and intensities of which were independent of chemical composition in the range $0{\cdot}67 < x < 1{\cdot}14$. At composition $x = 1$, strong dielectric absorption was found parallel to the tunnel direction. This was associated with the movement of Ba^{2+} ions towards adjacent empty cubes [on average half the cubic sites are filled (see Fig. 1*c*)]. They proposed that for $x = 1{\cdot}0$ all the tunnels are half-filled. At composition $x = 0{\cdot}67$ the ratio of Ba^{2+} to vacancies is

Table 1. *Atomic coordinates for hollandite (Byström & Byström, 1950)*

Space group: $I4/m(C_{4h}^5)$
Atomic positions: (000); $(\frac{1}{2}\frac{1}{2}\frac{1}{2})$ plus

$(2-y)\,A$ in $2(b)$: $00\frac{1}{2}$
$(8-z)\,B$ in $8(h)$: x_1y_10; $\bar{x}_1\bar{y}_10$; $\bar{y}_1x_10$; $y_1\bar{x}_10$
$8X$ in $8(h)$: x_2y_20; *etc.*
$8X$ in $8(h)$: x_3y_30; *etc.*,

where

$x_1 = 0{\cdot}348$	$x_2 = 0{\cdot}153$ (0·152)*	$x_3 = 0{\cdot}542$
$y_1 = 0{\cdot}167$	$y_2 = 0{\cdot}180$ (0·208)	$y_3 = 0{\cdot}167$ (0·152)

* Values in parentheses obtained by Dryden & Wadsley (1958) for $Ba_{1{\cdot}0}Mg_{1{\cdot}0}Ti_7O_{16}$.

1:2 but the absorption characteristics were virtually unchanged. They suggested that the sequence

$$Ba^{2+}\text{–vacancy–}Ba^{2+}\text{–vacancy}$$

must now be present along a certain fraction of the tunnels, giving identical dielectric absorption as for $x = 1{\cdot}0$, but that the remaining tunnels should be completely empty. Thus the non-stoichiometric phase $Ba_x(Ti_{8-x}Mg_x)O_{16}$ should contain different ratios of half-filled and completely empty tunnels for $0{\cdot}67 < x < 1{\cdot}14$. The sequences in adjacent tunnels need not be in phase with each other, giving rise to the observed almost structureless diffuse sheets in the diffraction patterns. Beyeler (1976) prepared a sample of $K^+_{1{\cdot}54}Mg^{2+}_{0{\cdot}77}Ti^{4+}_{7{\cdot}23}O_{16}$ which has approximately two thirds of the cubic sites filled. Comparison of X-ray diffuse scattering from this sample with a hollandite $K^+_{1{\cdot}54}Ti^{3+}_{1{\cdot}54}Ti^{4+}_{6{\cdot}46}O_{16}$ showed that the diffuse scattering does not depend upon the stoichiometry of the framework. Thus it originates exclusively from the potassium ions. The principal features of the diffuse scattering were a diffuse sheet situated at 0·22 reciprocal lattice units (rlu) (1 rlu = $2{\cdot}90^{-1}$ Å^{-1}) from the Bragg spots. The sheets had width approximately 0·08 rlu, which corresponds to a correlation length 35 Å, *i.e.* twelve channel sites. The diffuse scattering was analysed in terms of a supercell containing four channel sites, one of which was assumed empty, and the K^+ ions adjacent to the vacant site were allowed to have displacement x towards the hole. Random displacements of 2·90 Å (*i.e.* c_h) between adjacent channel sequences were required to produce thin diffuse sheets at $\frac{1}{4}$, $\frac{1}{2}$ and $\frac{3}{4}$ rlu between Bragg spots. The intensity of the diffuse scattering depends sensitively upon x and comparison with experiment, after also allowing random mixing of supercells of 2 × to 5 × 2·90 Å, gave $x = 0{\cdot}245$.

(*b*) *Structure of psilomelane*, $Ba_xMn_5O_{16}(2-x)H_2O$, $0{\cdot}50 < x < 0{\cdot}75$

This structure was determined by Wadsley (1953). Crystallographic parameters are $a_p = 9{\cdot}56$, $b_p = 2{\cdot}88$, $c_p = 13{\cdot}85$ Å, $\beta_p = 92°\,30'$.

The space group is $A2/m$ and the structure is illustrated in Fig. 2. The framework structure is again BX_2 but now contains both double and treble octahedral edge-shared strings. These intersect, forming junctions identical to the rutile-type columns indicated in Fig. 1(*a*), (*b*). The larger rectangular tunnels contain double rows of Ba^{2+} and H_2O. The crystal structure was solved by assuming these two substitute isomorphously for each other. The ideal ratio $Ba^{2+}:H_2O$ is 1:2. It was assumed, by analogy with hollandite, that order exists within any one tunnel which is uncorrelated with the ordering in adjacent tunnels. An ordering sequence was proposed whereby Ba^{2+} was bonded to four H_2O molecules, two in the adjacent row in the same tunnel and two adjacent sites in the same row, the tenfold coordination of the Ba^{2+} being completed with oxygens of the framework. This model provided for ready loss or gain of water. Variability of composition is achieved by replacement of Ba^{2+} by H_2O. Whether this occurs randomly or whether some tunnels are completely empty is unknown. Dehydration with the accompanying structural change to hollandite, occurs on heating at 823 K.

(*c*) *Ramsdellite structure type* (γ-MnO_2)

The mineral ramsdellite and γ-MnO_2 have the double-octahedral chain structure shown in Fig. 3(*a*). This is essentially the diaspore structure (Wells, 1975) except that the short O—O contacts of 2·65 Å due to

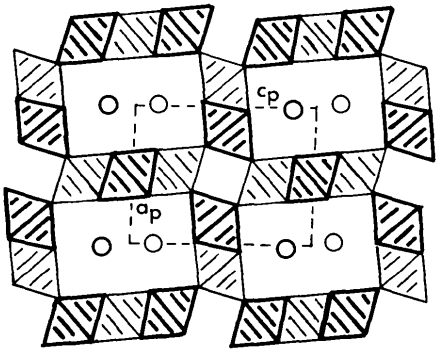

Fig. 2. The psilomelane structure, $[010]_p$ projection. Note triple edge-shared octahedral strings joined by corner-sharing to hollandite-type double-octahedral strings to form larger tunnels which may be occupied by Ba^{2+} and H_2O (circled).

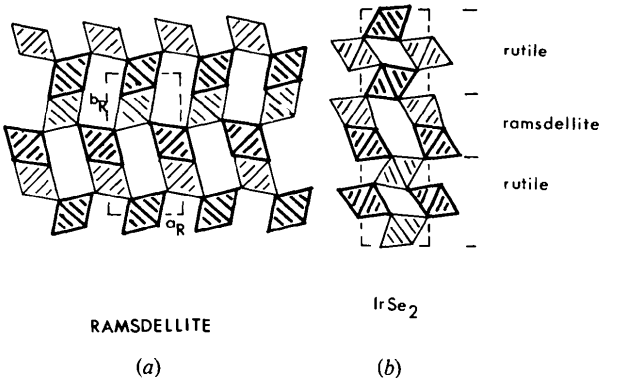

Fig. 3. (*a*) The ramsdellite structure, $[001]_r$ projection. Note double-octahedral strings, common to hollandite, psilomelane and β-gallia, joined in such a way as to produce double-square rectangular tunnels. Note antiphase boundary operation $(100)_r$, $[\frac{111}{242}]_r$ which relates rutile to ramsdellite. (*b*) Structure of $IrSe_2$, proposed for γ'-MnO_2, consisting of a periodic intergrowth of rutile and ramsdellite slabs.

hydrogen bonding in AlO.OH [also goethite FeO.OH, groutite MnO.OH and montroseite (V,Fe)O.OH] have lengthened to the normal value of 3·34 Å in ramsdellite (also paramontroeseite VO_2). This group of structures may be derived from rutile by the regularly repeated anti-phase (*AP*) operation $(100)_r[\frac{111}{242}]_r$ (Stone & Bursill, 1977). The collective name γ'-MnO_2 is given to a range of materials whose X-ray diffraction patterns suggest poorly crystalline material intermediate between ramsdellite and pyrolusite (β-MnO_2, rutile type). It has been suggested (de Wolff, 1959) that these γ' phases have the structure shown in Fig. 3(*b*). The latter is also the known structure of $IrSe_2$ (Hyde, Bagshaw, O'Keeffe & Andersson, 1974). Here the $(100)_r$ rutile slabs are sufficiently wide to be readily recognizable.

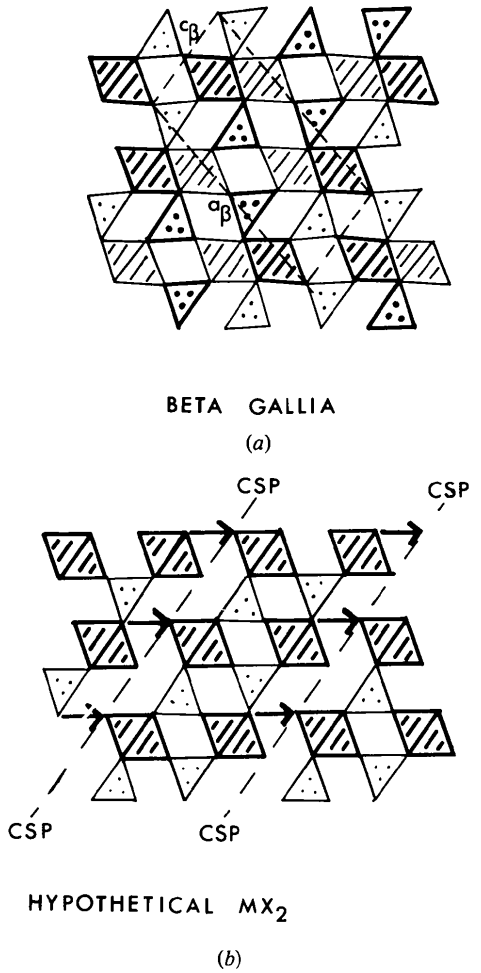

Fig. 4. (*a*) Structure of β-gallia, Ga_2O_3, $[010]_\beta$ projection. Note double-octahedral strings now joined by corner-sharing with $[GaO_4]$ tetrahedra. The anion array is almost perfect c.c.p. (*b*) MX_2 polymorph (hypothetical) consisting of equal numbers of filled octahedral and tetrahedral sites in a c.c.p. array of anions. β-Gallia may be derived from this by a *CS* operation as indicated.

(*d*) *Rutile structure*

This consists of strings of edge-shared $[TiO_6]$ octahedra joined by corner-sharing as shown in the $[001]_r$ projection (Fig. 1*a*). The topology of the anions is often idealized to h.c.p. but Hyde, Bagshaw, O'Keeffe & Andersson (1974) have pointed out that the anion array is in fact intermediate between h.c.p. and c.c.p.

(*e*) *β-gallia structure*

The high-temperature form of gallia (β-Ga_2O_3) has an anion array which is almost perfect c.c.p. Cell parameters are (Geller, 1960) $a_\beta = 12{\cdot}23$, $b_\beta = 3{\cdot}04$, $c_\beta = 5{\cdot}80$ Å, $\beta_\beta = 103{\cdot}7°$, and the space group is $C2/m$. The $[010]_\beta$ projection (Fig. 4*a*) shows the same double-edge shared strings as occur in hollandite, psilomelane and ramsdellite. These are joined together by corner-sharing to $[GaO_4]$ tetrahedra. Equal numbers of filled octahedral and tetrahedral sites occur per unit cell, dotted in Fig. 4(*a*). Hyde, Bagshaw, O'Keeffe & Andersson (1974) also noted that the $(100)_r$ $[\frac{111}{242}]_r$ *AP* operation in rutile introduces an element of the c.c.p. anion array at the boundary. If the rutile anion array is idealized to c.c.p. then alternate $(100)_r$ layers of cations may be shuffled by a very small vector normal to c_r, falling into tetrahedral coordination. This gives another BX_2 framework (Fig. 4*b*). This may then be related to β-gallia by a crystallographic shear operation, as indicated in Fig. 4.

(*f*) *Gallium titanate structures*, $Ga_4Ti_{m-4}O_{2m-2}$, *m odd.*

The structure of $Ga_4Ti_{21}O_{48}$ is shown projected along the short (*i.e.* 2·96 Å) axis in Fig. 5. Cell parameters and atomic coordinates are given in Lloyd, Grey & Bursill (1976). The two metal atom sites which together contain over 80% of the gallium have their coordination polyhedra heavily outlined.

Comparison with β-gallia (Fig. 4*a*) shows that $Ga_4Ti_{21}O_{48}$ is a coherent intergrowth, parallel to $(210)_r$, of the rutile structure with columns of the β-gallia structure. (In β-gallia Ga occupies both the octahedral and tetrahedral sites.) However, the disposition of adjacent columns differs in the two structures. It is necessary to rotate alternate β-gallia-like columns of Fig. 4(*a*) by 180° and expand them slightly to generate the outlined structure of $Ga_4Ti_{21}O_{48}$. The β-gallia-like columns are separated by large tunnels of hexagonal outline, having periodicity 10·3 Å and effective diameter 2·5 Å. An atom situated in the tunnels would have ninefold coordination to oxygens with $B-X$ distances from 2·3 to 2·8 Å.

Across the $(210)_r$ boundary, adjacent rutile blocks are displaced by $[\frac{111}{242}]_r$. Note also that the puckered $(100)_r$ anion layers are considerably flattened towards

ideal c.c.p. It is interesting that in gallia-doped rutile defect-pairs of $(210)_r$ boundaries occur rather than the isolated crystallographic shear planes shown in Fig. 5(*a*). These have been directly imaged by high-resolution (3·2 Å) electron microscopy (Stone & Bursill, 1977) and have the structure shown in Fig. 5(*b*). It appears that β-Ga_2O_3 reacts chemically with TiO_2 to form Ga_4TiO_8 ($m = 5$ is the lowest m value in the series $Ga_4Ti_{m-4}O_{2m-2}$) coherently intergrown with rutile. Ga_4TiO_8 is also closely related to β-gallia. If adjacent $(001)_\beta$ slabs of β-gallia are displaced by $[\frac{1}{2}0\frac{1}{2}]_\beta$, a slab of $[TiO_6]$ octahedra separated by hexagonal tunnels may be inserted to produce Ga_4TiO_8. The formation of the $(210)_r$ defect-pairs must therefore be regarded as a chemical defect representing one half of the diffusion couple produced between TiO_2 and Ga_2O_3. Thus there is the possibility of a gallia-rich family of structures $TiGa_{4n}O_{6n+2}$ between the end members Ga_2O_3 and Ga_4TiO_8. It is significant that the $(210)_r$ defect-pairs, or Ga_4TiO_8, may be described as derived from rutile by the *CS* operation $(210)_r\,[\frac{1}{2}\frac{1}{4}\frac{1}{2}]_r$ or, alternatively, by the *CS* operation $(001)_\beta\,[\frac{1}{2}0\frac{1}{2}]$ on β-gallia. The displacement vector $[\frac{1}{2}\frac{1}{4}\frac{1}{2}]_r$ acting across $(100)_r$ of rutile would eliminate a slab of stoichiometry TiO_2. We have therefore predicted the existence of a new family of swinging crystallographic shear structures having indices $(hkl)_r$ between $(210)_r$ and $(100)_r$ given by

$$(hkl)_r = p(210)_r + q(100)_r,$$

where p,q are integers (*cf.* Bursill, Hyde & Philp, 1971). Addition of MnO_2 to the TiO_2–Ga_2O_3 system may provide the key to the formation of such structures. Fig. 6(*a*) shows the antiphase operation $(100)_r[\frac{1}{2}\frac{1}{4}\frac{1}{2}]_r$ which is essentially intergrowth of ramsdellite and rutile. In fact we have been able to induce such defects to occur in MnO_2-doped rutile (Bursill & Stone, 1979*b*). Fig. 6(*b*) shows a model for the $(310)_r$ $[\frac{1}{2}\frac{1}{4}\frac{1}{2}]_r$ *CS* structure, where elements of β-gallia and ramsdellite structure alternate along the *CSP*. Further structural models, for the splitting and sideways movement of $(210)_r$ *CSP*, and for the dislocation structure at the termination of a Ga_4TiO_8 defect-pair inside a rutile matrix, have been given by Stone & Bursill (1977). The latter (Fig. 6*c*) contains only elements of ramsdellite and β-gallia in the 'dislocation core' region (Burgers vector $[0\frac{1}{2}0]_r$).

3. New structural relationships

(*a*) *Generation of hollandite-type tunnels by intersecting* $(100)_r[\frac{1}{2}\frac{1}{4}\frac{1}{2}]_r$ *and* $(010)_r[\frac{1}{4}\frac{1}{2}\frac{1}{2}]_r$ *boundaries*

In Fig. 7(*a*) we show that the large hollandite tunnel may be generated in rutile at the junction of orthogonal $(100)_r[\frac{1}{2}\frac{1}{4}\frac{1}{2}]_r$ and $(010)_r[\frac{1}{4}\frac{1}{2}\frac{1}{2}]_r$ *AP* boundaries. This leads to an alternative mechanism for transformation from rutile to hollandite. By repeated operation of such intersections we may generate the hollandite framework (Fig. 7*b*). Of course, many intermediate structures may occur having tetragonal or orthorhombic symmetry by varying the spacings of the antiphase boundaries, see Fig. 7(*c*),(*d*) for examples. Fig. 7(*d*) also shows examples of possible disordered intermediate stages.

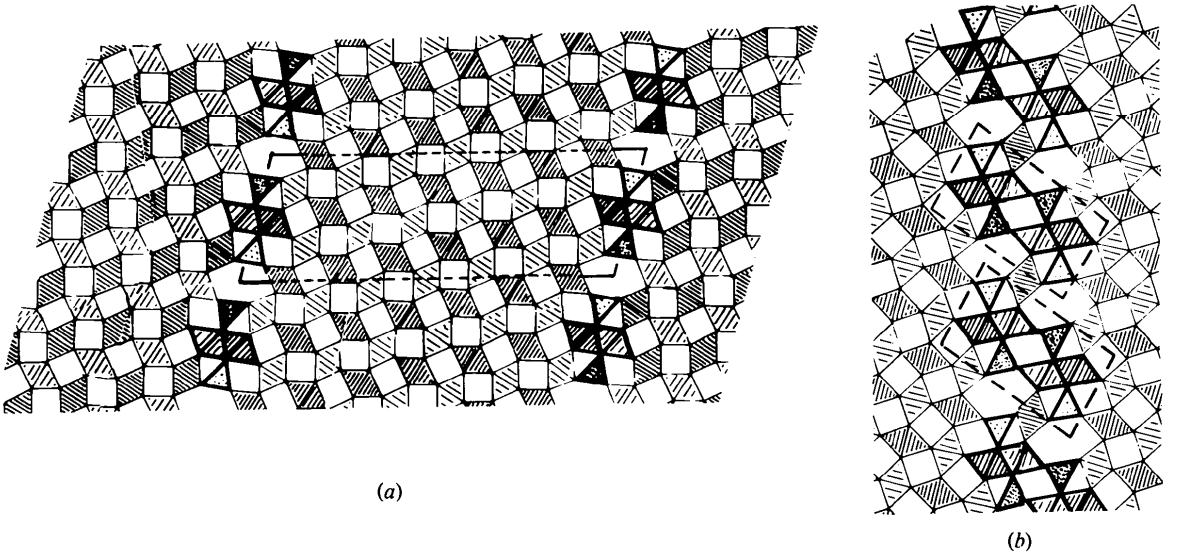

(*a*) (*b*)

Fig. 5. (*a*) Structure of gallium titanate, $Ga_4Ti_{21}O_{48}$, $[010]_r$ projection. Note β-gallia-type columns (heavily outlined) occurring at $(210)_r$ $[\frac{1}{2}\frac{1}{4}\frac{1}{2}]_r$ *CS* planes. These are separated by empty tunnels having hexagonal outline. Note short segments of c.c.p. anions at the *CS* planes. (*b*) Ga_4TiO_8 $(210)_r$ defect-pair in rutile matrix : β-gallia elements larger than in (*a*) are indicated.

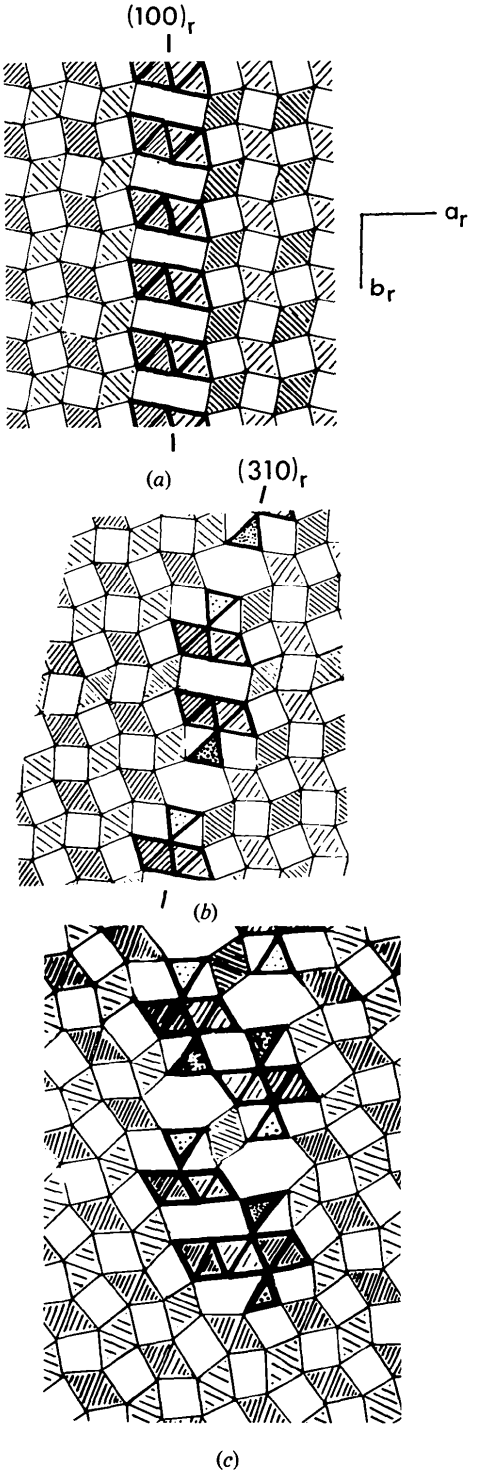

Fig. 6. (*a*) The antiphase (*AP*) operation $(100)_r\ [\frac{1}{2}\frac{1}{2}\frac{1}{2}]_r$ in rutile, generating intergrowth slabs of rutile and ramsdellite. (*b*) Formation of $(310)_r\ [\frac{1}{2}\frac{1}{2}\frac{1}{2}]_r$ *CS* boundary by intergrowth of $(210)_r$ + $(100)_r$ β-gallia and ramsdellite units. (*c*) Dislocation core structure at termination of Ga_4TiO_8 defect-pair in rutile matrix. Note element of triple edge-shared octahedral strings and ramsdellite-type tunnel.

The unit cells of these structures may be related to that of rutile by the matrix

$$\begin{pmatrix} a'_h \\ b'_h \\ c'_h \end{pmatrix} = \begin{pmatrix} m & 0 & 0 \\ 0 & n & 0 \\ 0 & 0 & l \end{pmatrix} \begin{pmatrix} a_r \\ b_r \\ c_r \end{pmatrix}$$

where m, n are integers, representing the *AP* boundary spacings in units of a_r (= 4·6 Å). A further crystallographic shear (*CS*) operation of $(100)_r\ [0\frac{1}{2}\frac{1}{2}]_r$ converts the hollandite-type tunnels into psilomelane-type (Fig. 8*a*). Again, myriad possibilities exist for generation of structures consisting of intergrowths of hollandite- and psilomelane-type frameworks, for example see Fig. 8(*b*).

(*b*) *Hollandite and even larger tunnels generated by intersecting* $(210)_r\ [\frac{1}{2}\frac{1}{4}\frac{1}{2}]_r$ *and* $(\bar{1}20)_r\ [\frac{1}{4}\frac{1}{2}\frac{1}{2}]_r$ *CSP*

Structures containing both hollandite- and gallium titanate-type tunnels may be simply generated by considering the intersection of $(210)_r\ [\frac{1}{2}\frac{1}{4}\frac{1}{2}]_r$ and $(\bar{1}20)_r\ [\frac{1}{4}\frac{1}{2}\frac{1}{2}]_r$ *CSP* in rutile. Fig. 9(*a*) for example shows two such orthogonal faults. Note the large square hollandite tunnel generated at the junction. Fig. 9(*b*) shows that an even larger tunnel is generated at the intersection of two orthogonal Ga_4TiO_8 defect-pairs. This is larger than the tunnel found in psilomelane. It also contains elements of the ramsdellite structure. (Direct evidence for such a tunnel is given by Bursill & Stone, 1979*a*.) Ordered and disordered structures having tunnels of the types shown in Fig. 9(*a*),(*b*) may easily be generated by repeating the intersections at regular or irregular intervals.

(*c*) *Intersection of* $(210)_r\ [\frac{1}{2}\frac{1}{4}\frac{1}{2}]_r$ *and* $(010)_r\ [\frac{1}{4}\frac{1}{2}\frac{1}{2}]_r$ *CSP*

An example of such an intersection is given in Fig. 10. Note that in this case the hollandite-type tunnel is not square but a parallelogram. It could easily be filled by placing a string of anions at the centre of the tunnel which generates strings of tetrahedral sites (Fig. 10), completing β-gallia-type units. In Fig. 10 the *APB* operation $(010)_r\ [\frac{1}{4}\frac{1}{2}\frac{1}{2}]_r$ has been applied to $Ga_4Ti_7O_{20}$. It could equally well be applied to any member $Ga_4Ti_{m-4}O_{2m-2}$ (m odd) to generate ordered or disordered structures. The variety of structures is extended by allowing either large *B* anions or $[MO_4]$ tetrahedra to occupy the tunnels.

(*d*) *Intergrowth of hollandite and* β*-gallia*

Fig. 11(*a*) shows that there is a very close topological relationship between these two structures with

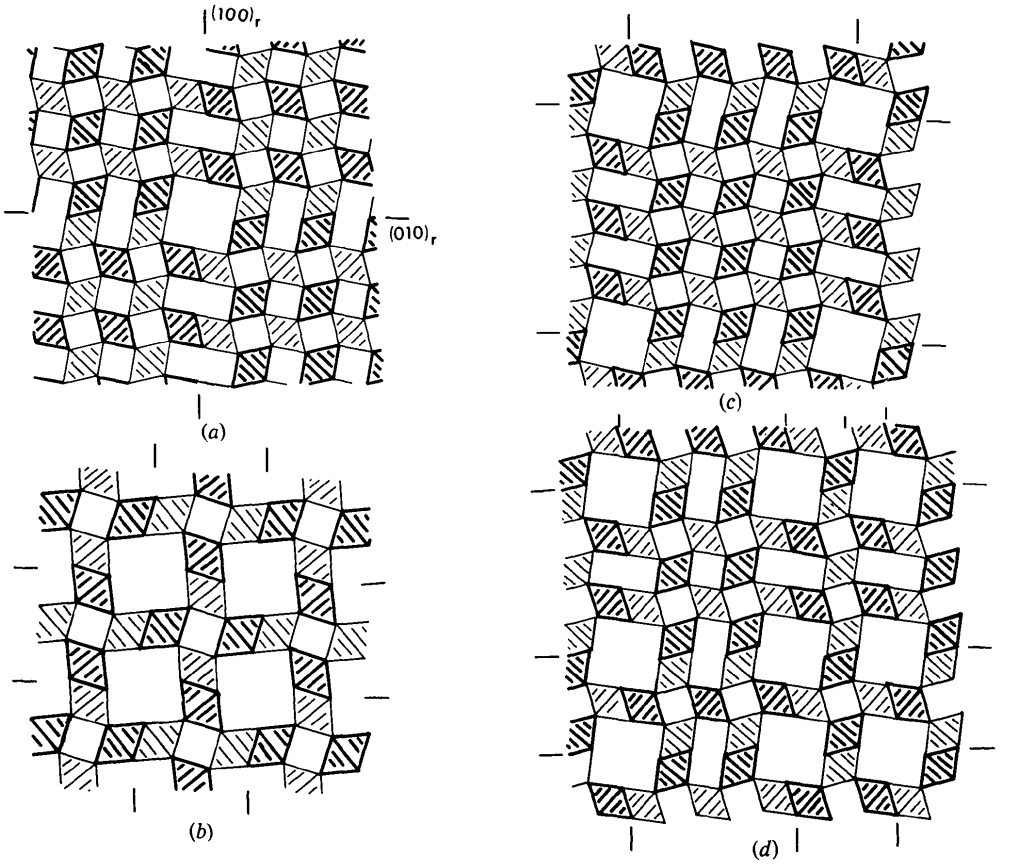

Fig. 7. (*a*) Formation of hollandite-type square tunnel at junction of $(100)_r$ $[\frac{1}{2}\frac{1}{2}\frac{1}{2}]_r$ and $(010)_r$ $[\frac{1}{2}\frac{1}{2}\frac{1}{2}]_r$ *AP* boundaries in rutile matrix. (*b*) Repeated periodic operation of operation shown in (*a*) generates the hollandite BX_2 framework. (*c*) Hollandite-type tunnels separated by larger rutile columns, produced by two orthogonal *AP* boundary operations. (*d*) Disordered structure having mixture of tunnel spacings.

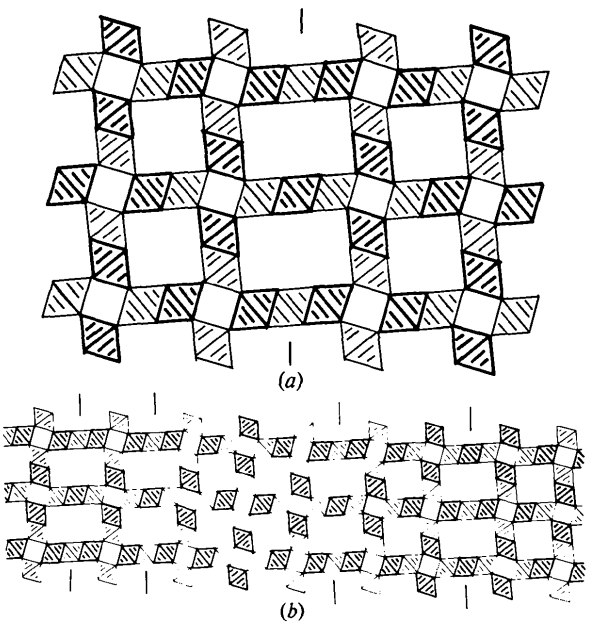

Fig. 8. (*a*) Formation of psilomelane framework from hollandite by *CS* operation $(100)_h$ $[0\frac{1}{2}0]_h$. (*b*) Disordered intergrowth of hollandite and psilomelane type tunnels.

$(110)_h \| (100)_\beta$ and $(001)_h \| (010)_\beta$. The square tunnels at the interface could alternatively be occupied by $[MO_4]$ tetrahedral strings (Fig. 11*b*), again naturally pushing over the hollandite tunnels (*cf.* Fig. 10). Indeed, many further variations of the hollandite framework may be imagined, depending on whether *A* or $[MO_4]$ occupy the tunnels and upon the spacing of the square tunnels. One might expect that if all of the tunnels are empty the hollandite structure would deform as shown in Fig. 11(*c*).

(*e*) *Intergrowth of rutile, β-gallia and hollandite*

Even more elaborate tunnel structures may be derived containing these three structures. Fig. 12 shows for example a structural model required for matching observed images and diffraction patterns for a phase in the BaO–Ga_2O_3–TiO_2 system. Note that two orthogonal elements of the β-gallia structure are required. These link in such a way as to complete hollandite-type square tunnels, leaving space for just one column of four rutile octahedral strings between the β-gallia units.

4. Conclusion

The above discussion of the relationships between rutile, β-gallia, hollandite, ramsdellite, psilomelane and the gallium titanates is important for the following reasons.

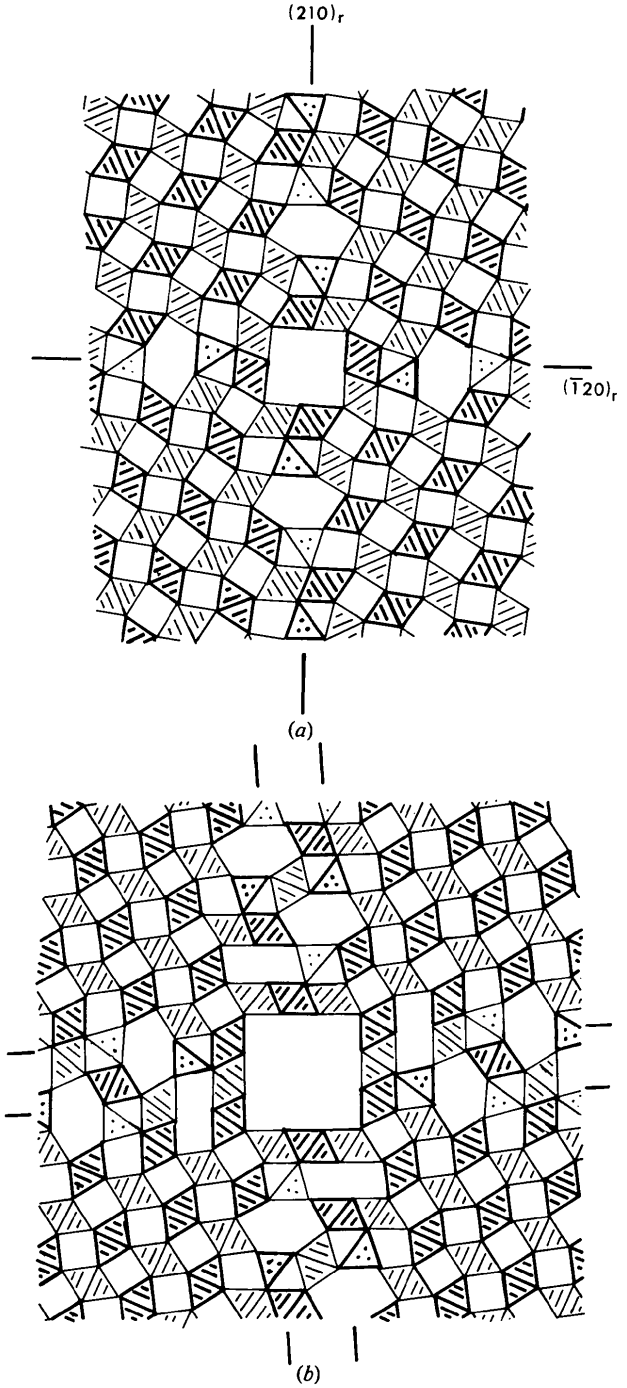

Fig. 9. (*a*) Hollandite tunnel produced by intersection of orthogonal $(210)_r$ $[\frac{1}{2}\frac{1}{2}\frac{1}{2}]_r$ and $(\bar{1}20)_r$ $[\frac{1}{4}\frac{1}{2}\frac{1}{2}]_r$ *CS* planes. (*b*) Larger tunnel, containing triple edge-shared octahedral strings, produced at the intersection of Ga_4TiO_8 defect pairs in a rutile matrix.

(1) It predicts that there should be many more variations on the hollandite-type structure than were previously suspected. This should lead, after further experimental work, to a complete understanding of the so far indefinite structural results obtained by Byström & Byström (1950). Clearly the close relationship between the structures and the known variable stoichiometry of minerals would combine to make natural hollandites and γ-manganese oxides/hydroxides virtually impossible to characterize by X-ray diffraction alone.

(2) The probable importance of the tunnel structures, such as hollandite, psilomelane and the new structure proposed in Fig. 9(*b*) for use as superionic conductors suggests that preparative and characterization techniques (see for example Singer, Kautz, Fielder & Fordyce, 1973) used for measurement of physical properties, such as ionic conductivity, need to be far more thorough and penetrating than those used to date.

(3) The realization that tunnel structures may be generated by intersecting *CS* boundaries provides a satisfying theoretical link between these two important mechanisms for accommodation of stoichiometry changes. The double *CS* mechanism resembles block

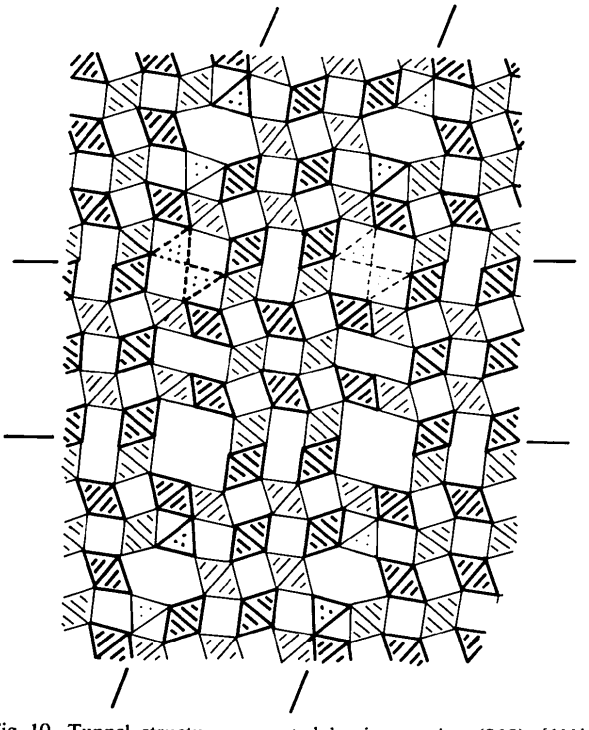

Fig. 10. Tunnel structure generated by intersecting $(210)_r$ $[\frac{1}{2}\frac{1}{2}\frac{1}{2}]_r$ and $(010)_r$ $[\frac{1}{4}\frac{1}{2}\frac{1}{2}]_r$ boundaries {$(010)_r$ $[\frac{1}{4}\frac{1}{2}\frac{1}{2}]_r$ is applied to $Ga_4Ti_7O_{20}$}. Note that in this case the large tunnels are not square but deformed. These may be occupied by large *A* ions. Filling of large tunnels (dotted) by $[GaO_4]$ tetrahedral strings is an alternative possibility.

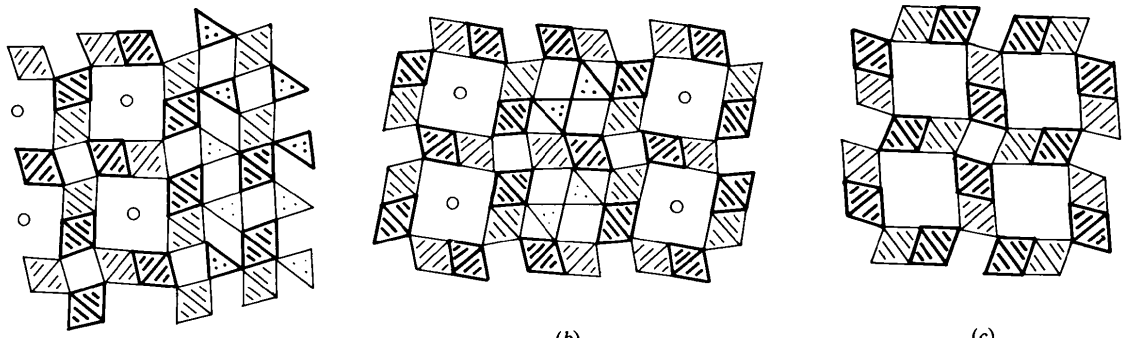

Fig. 11. (*a*) Topotaxy between hollandite and β-gallia type structures with $(110)_h \| (100)_\beta$ and $(001)_h \| (010)_\beta$. (*b*) Same as (*a*) except that $[GaO_4]$ tetrahedral strings replace large *A* ion in half of the tunnels, producing oblique axes at 95°. (*c*) Empty hollandite framework showing possible deformation of large tunnels, based upon relationship to β-gallia of Fig. 10.

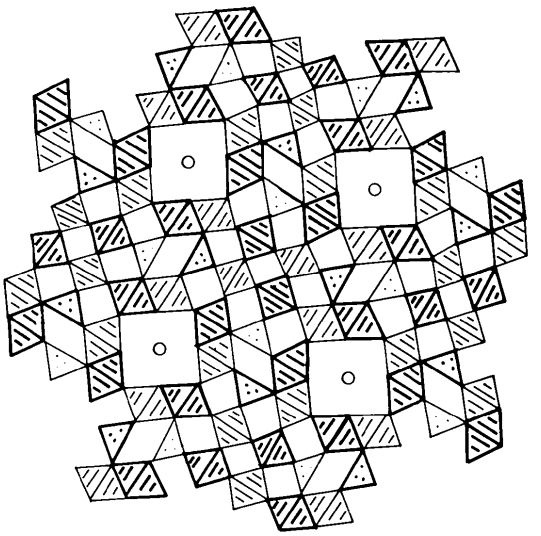

Fig. 12. Complex intergrowth of rutile, hollandite and β-gallia structure elements. Note two orthogonal (twin-related) elements of β-gallia link to form hollandite-like tunnels. Rutile occupies interstices between β-gallia units.

structure mechanisms (see for example Bursill, 1973) and provides an attractive alternative to rotation-type operations (Fig. 1). It should be interesting to observe one or other of these mechanisms occurring *in situ* in the electron microscope.

This work was supported financially by the Australian Research Grants Committee and the University of Melbourne.

References

BEYELER, H. U. (1976). *Phys. Rev. Lett.* **37**, 1557–1560.
BURSILL, L. A. (1973). *J. Solid State Chem.* **6**, 195–202.
BURSILL, L. A. & HYDE, B. G. (1972). *Nature (London) Phys. Sci.* **240**, 122–124.
BURSILL, L. A., HYDE, B. G. & PHILP, D. K. (1971). *Philos. Mag.* **23**, 1501–1513.
BURSILL, L. A. & NETHERWAY, D. J. (1979). *Acta Cryst.* To be submitted.
BURSILL, L. A. & STONE, G. G. (1979*a*). *Acta Cryst.* To be submitted.
BURSILL, L. A. & STONE, G. G. (1979*b*). *Philos. Mag.* To be submitted.
BURSILL, L. A. & WILSON, A. R. (1977). *Acta Cryst.* A**33**, 672–676.
BUSER, W., GRAF, P. & FEITKNECHT, W. (1954). *Helv. Chim. Acta*, **37**, 2322–2333.
BYSTRÖM, A. & BYSTRÖM, A. M. (1950). *Acta Cryst.* **3**, 146–154.
DRYDEN, J. S. & WADSLEY, A. D. (1958). *Trans. Faraday Soc.* **54**, 1574–1580.
GELLER, S. (1960). *J. Chem. Phys.* **33**, 676–684.
HYDE, B. G., BAGSHAW, A. N., O'KEEFFE, M. & ANDERSSON, S. (1974). *Annu. Rev. Mater. Sci.* **4**, 43–92.
LLOYD, D. J., GREY, I. E. & BURSILL, L. A. (1976). *Acta Cryst.* B**32**, 1756–1761.
SINGER, J. S., KAUTZ, H. E., FIELDER, W. L. & FORDYCE, J. S. (1973). *Fast Transport in Solids*, edited by W. VAN GOOL, pp. 653–663. Amsterdam: North-Holland.
STONE, G. G. & BURSILL, L. A. (1977). *Philos. Mag.* **35**, 1397–1412.
WADSLEY, A. D. (1953). *Acta Cryst.* **6**, 433–438.
WADSLEY, A. D. (1964). *Non-Stoichiometric Compounds*, edited by L. MANDELCOIN, p. 111. New York: Academic Press.
WADSLEY, A. D. & WALKLEY, A. (1951). *Rev. Pure Appl. Chem.* **1**, 203–213.
WELLS, A. F. (1975). *Structural Inorganic Chemistry*, 4th ed., p. 526. Oxford: Clarendon Press.
WOLFF, P. M. DE (1959). *Acta Cryst.* **12**, 341–346.